IEICE TRANS. ELECTRON., VOL.E97–C, NO.8 AUGUST 2014

BRIEF PAPER

Accurate Target Extrapolation Method Exploiting Double Scattered Range Points for UWB radar

Ayumi YAMARYO[†a)], ***Student Member***, **Shouhei KIDERA**[†], ***and*** **Tetsuo KIRIMOTO**[†], ***Members***

SUMMARY Ultra-wide band (UWB) radar has a great advantage for range resolution, and is suitable for 3-dimensional (3-D) imaging sensor, such as for rescue robots or surveillance systems, where an accurate 3-dimensional measurement, impervious to optical environments, is indispensable. However, in indoor sensing situations, an available aperture size is severely limited by obstacles such as collapsed furniture or rubles. Thus, an estimated region of target image often becomes too small to identify whether it is a human body or other object. To address this issue, we previously proposed the image expansion method based on the ellipse extrapolation, where the fitting space is converted from real space to data space defined by range points to enhance the extrapolation accuracy. Although this method achieves an accurate image expansion for some cases, by exploiting the feature of the efficient imaging method as range points migration (RPM), there are still many cases, where it cannot maintain sufficient extrapolation accuracy because it only employs the single scattered component for imaging. For more accurate extrapolation, this paper extends the above image expansion method by exploiting double-scattered signals between the target and the wall in an indoor environment. The results from numerical simulation validate that the proposed method significantly expands the extrapolated region for multiple elliptical objects, compared with that obtained using only single scattered signal.

key words: *UWB radar, Range points migration, Ellipse fitting, Double scattered signal*

1. Introduction

UWB radar has a great potential to create an innovative short-range sensing technique, because it has a high range resolution at the order of cm and a penetration ability of dielectric objects such as walls. Thus, UWB radar can provide an essential solution for robotic or security sensing issue, because it is impervious to a harsh optical environment, such as thick smog or strong backlight. As one of the most efficient 3-dimensional (3-D) imaging approaches aimed at indoor environments, the range points migration (RPM) method has been established [1], [2] where the 3-D target boundary image is accurately reconstructed with much less computation time compared with the former beam forming or synthetic aperture radar (SAR) schemes [3]. In addition, RPM is widely extended to various situations, such as moving target estimation [4] or complex-shaped target reconstruction in indoor environments [5]. However, the image region obtained by the RPM or other typical radar imaging methods is strictly determined by the equivalent aperture size, and it is often incapable of identifying target shape, especially when the object is far from the observation site because obstacles such as rubble are present within the disaster zone.

To address the above issues, the efficient image extrapolation method has been developed [6]. Assuming that the head and limbs of a human body are roughly approximated to an ellipsoid, the method [6] adopts ellipse fitting in the data space comprising antenna location and observed range points. This is because ellipse fitting in real space namely for the obtained image by RPM is too sensitive to imaging errors. This method only employs the RPM for image clustering and the fitting process is directly carried out without through RPM process; thus, it is essentially impervious to the RPM imaging error. Although it has been verified that the method [6] accomplished accurate target extrapolation in noise situations, this method has a serious drawback that its accuracy is still insufficient, especially when an estimated target image by RPM expresses only a tiny part of ellipse. This is an inherent problem as far as only a single scattered signal is used for imaging or extrapolation.

As a solution for this difficulty, this paper proposes the image expansion method exploiting the double-scattered signals generated between wall and target. A number of investigations have already verified that the double-scattered signal is useful for image expansions [7], [8] because this component includes independent information of the scattering point from that obtained by single-scattered component. Assuming the receiving antenna is located at the mirror image of the transmitting antenna, the RPM method is readily extended to the bi-static model to deal with the double-scattered signal. In addition, the appropriate clustering process for the image reproduced by single- or double-scattered signals is introduced. This clustering process also aids in suppressing false images generated by other multiple-scattered components. The results from numerical simulations of indoor environments show that the proposed method significantly expands the target image even under noisy conditions.

2. System Model

Figure 1 shows the system model. A mono-static radar signal with omni-directional antenna is scanned in a circular path. Note that any curvilinear scan is acceptable in the method introduced in this study. To obtain identical aperture sizes for all directions of exiting targets, circular scans are adopted here. Each target is assumed elliptical with sharp

Manuscript received August 20, 2013.
Manuscript revised February 19, 2014.

[†]The authors are with Graduate School of Informatics and Engineering, University of Electro-Communications, Tokyo, Japan.
a) E-mail: yamaryo@secure.ee.uec.ac.jp

DOI: 10.1587/transele.E97.C.828

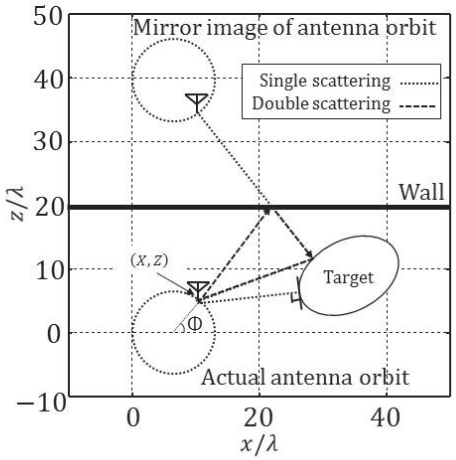

Fig. 1 System model.

boundaries. A wall boundary is located at $z = Z_{\text{wall}}$; internal reflections are not considered ; specifically, it is assume to be a perfect electric conductor material. The transmitted signal is composed of a mono-cycle pulse with center wavelength λ where the nominal range resolution is around 0.235λ in the standard of half-value width for an envelope of the transmitted signal. The points in coordinate space, in which the target and antenna are located, is expressed by parameters (x, z). $s(X, Z, R)$ is the output of the Wiener filter for the signal received at the location $(x, z) = (X, Z)$, where $R = c\tau/2\lambda$ with τ defined as the delay time and c the speed of the radio wave. For simplicity, higher order scattering above third order is not considered. $\boldsymbol{q}_S = (X, Z, R_S)$ and $\boldsymbol{q}_D = (X, Z, R_D)$ are each defined as the range point corresponding to the scattering center reflected by the respective single- or double-scattered signals, which are determined by the geometrical optics approximation. Specifically, they are extracted from the local maximum or local minimum of $s(X, Z, R)$ because the phase between single- and double-scattered signals becomes 180° out of phase; details are described in [7].

3. Conventional Method

In [6], we proposed the range-points-based ellipse extrapolation method and demonstrated it as one of the most promising ellipse-fitting approaches. For comparison with the proposed method, this section briefly explains its principle and methodology. In major approaches to ellipse fitting, one predicts that fitting scheme in the real space, where each estimated image after clustering is directly employed for ellipse fitting. It has been reported that the RPM accomplishes accurate and robust target imaging, but when an obtained target image is too small to reconstruct the whole target shape, quite small imaging errors in the RPM process become fatal in such extrapolations. Thus, the fitting scheme based on the target points (namely, in real space) is too sensitive to RPM imaging errors. To resolve this sensitivity, method [6] introduces range-point-based ellipse fitting, which is substantially unaffected by RPM image processing, because the fitting scheme is directly performed in data space.

First, the target points are reproduced using the RPM method with the extracted range points denoted as $\boldsymbol{q}_S$. Second, to classify the estimated target points into multiple ellipse objects, each estimated target point is clustered according to its Euclidean distance. Here, we define $\boldsymbol{P}_i = (a_i, b_i, X_{c,i}, Y_{c,i}, \theta_i)$ as parameters of the i-th ellipse whose major axis is a, minor axis is b, center between focal points is (X_c, Y_c), and angle from the x axis to the major axis is θ. Then, optimizing each $\hat{\boldsymbol{P}}_i$ for the i-th cluster is determined from

$$\hat{\boldsymbol{P}}_i^{\text{S}} = \arg\min_{\boldsymbol{P}} \sum_{\boldsymbol{q}_{S,i,k} \in Q_{S,i}}^{N_{S,i}} \left| R_{S,k,i} - R_{S,k}(\boldsymbol{P}; X_{k,i}, Z_{k,i}) \right|^2, \tag{1}$$

where $\boldsymbol{q}_{S,i,k}$ denotes the range point corresponding to the k-th target point in the i-th cluster, $Q_{S,i}$ is the set of range points corresponding to the i-th clustered target points, and $N_{S,i}$ denotes the total number of estimated range points in the i-th cluster using the single-scattered signal. $R_{S,k}(\boldsymbol{P}; X_{k,i}, Z_{k,i})$ denotes the minimum distance from $(X_{k,i}, Z_{k,i})$ to the ellipse expressed by $\boldsymbol{P}$.

Because this method substantially avoids degradation in ellipse fitting caused by RPM imaging errors, it enhances the robustness and accuracy in ellipse extrapolation compared to that obtained using ellipse fitting in real space. However, its accuracy is often insufficient when the reconstructed region is too small to describe the full target shape, because this method only employs single-scattered signals for the extrapolation.

4. Proposed Method

To avoid the difficulty just described, this section describes an novel image expansion method that exploits double-scattered signals generated between wall and target. There are a number of reports that the double-scattered signal has a great potential for enhancing the equivalent aperture size [7] because the propagation path of double-scattered wave is, in general, different from that of the single-scattered wave. In particular, double scattering is regarded as a single scattering where the transmitting location is the mirror position of the actual antenna ($(X, 2Z_{\text{wall}} - Z)$ in this case) of a wall and the receiving location is to the actual antenna (X, Z).

To deal with this type of double-scattered wave appropriately, we apply the RPM extended to the bi-static model [7] to range points obtained as $\boldsymbol{q}_{\text{D}}$, whereas the range points $\boldsymbol{q}_{\text{S}}$ are converted to target points by the mono-static RPM. After this imaging process, each target point is clustered to each ellipse based on the Euclidean distance; a similar approach is detailed in [7]. Similar to the conventional approach, this method introduces a fitting scheme in data space to avoid influences arising from imaging errors using the RPM method. The optimal ellipse parameter $\boldsymbol{P}^{\text{M}}$ of $\hat{\boldsymbol{P}}_i$ for the i-th cluster is then determined as

$$\hat{\boldsymbol{P}}_i^{\text{M}} = \arg\min_{\boldsymbol{P}} \quad \sum_{\boldsymbol{q}_{S,i,k} \in Q_{S,i}}^{N_{S,i}} \left| R_{S,k,i} - R_{S,k}(\boldsymbol{P}; X_{k,i}, Z_{k,i}) \right|^2$$

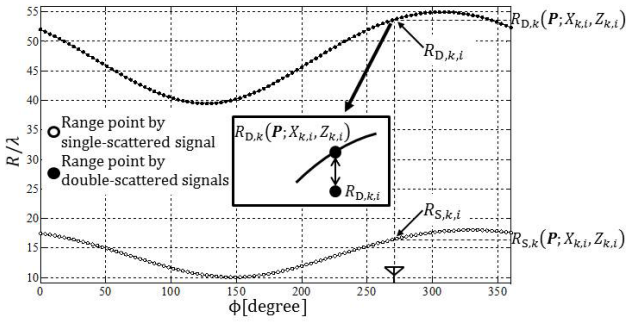

Fig. 2 Ellipse fitting for proposed method.

$$+\sum_{\boldsymbol{q}_{\mathrm{D},i,k}\in Q_{\mathrm{D},i}}^{N_{D,i}}\left|R_{\mathrm{D},k,i}-R_{\mathrm{D},k}(\boldsymbol{P};X_{k,i},Z_{k,i})\right|^2, \quad (2)$$

where $\boldsymbol{q}_{\mathrm{D},i,k}$ denotes the range point corresponding to the k-th target point in the i-th cluster, $Q_{\mathrm{D},i}$ is the set of range points corresponding to the i-th clustered target points. $R_{\mathrm{D},k}(\boldsymbol{P};X_{k,i},Z_{k,i})$ denotes the minimum distance from $(X_{k,i},Z_{k,i})$ through the wall to the ellipse expressed by $\boldsymbol{P}$ and $N_{\mathrm{D},i}$ denotes the total number of the estimated range point in the i-th cluster from double-scattered signals. Figure 2 shows the example of the ellipse fitting in data space, where Φ denotes the angle corresponding to antenna location as indicated in Fig. 1.

The procedure for the proposed method is summarized as follows.

Step 1). A sum of a set of estimated target points $\mathcal{T}_{\mathrm{S}}$ and $\mathcal{T}_{\mathrm{D}}$ are obtained by applying the mono-static RPM to $\boldsymbol{q}_{\mathrm{S}}$ by extracting from the local maximum of $s(X,Z,R)$ and the bi-static RPM to $\boldsymbol{q}_{\mathrm{D}}$ by extracting from the local minimum of $s(X,Z,R)$, respectively.

Step 2). $\mathcal{T}_{\mathrm{S}}$ and $\mathcal{T}_{\mathrm{D}}$ are clustered independently. The two nearest estimated target points in $\mathcal{T}_{\mathrm{S}}$ and $\mathcal{T}_{\mathrm{D}}$ are recursively combined as one cluster, until the distance for all pairs of clusters satisfies $D_{i,j} \geq \gamma$, where the constant γ is empirically determined. $D_{i,j}$ denotes the distance between the two clusters, which is defined in [9]. The i-th cluster of $\mathcal{T}_{\mathrm{S}}$ is denoted $C_{\mathrm{S},i}$ and j-th cluster of $\mathcal{T}_{\mathrm{D}}$ denoted $C_{\mathrm{D},j}$.

Step 3). For each cluster of $C_{\mathrm{D},j}$, the matching cluster of $C_{\mathrm{S},i}$ is determined using the same criteria in Step 2). Next, the $C_{\mathrm{D},j}$ is redefined as $C_{\mathrm{D}}(C_{\mathrm{S},i})$. Here, the cluster with smaller target points is removed as a false target image; details are described in [6].

Step 4). $\boldsymbol{P}$ is determined in Eq. (2), where $Q_{\mathrm{S},i}$ denotes the range point corresponding to the cluster $C_{\mathrm{S},i}$ and $Q_{\mathrm{D},i}$ denotes the range point corresponding to the $C_{\mathrm{D}}(C_{\mathrm{S},i})$.

Figure 3 depicts a flowchart of the proposed method.

5. Performance Evaluation in Numerical Simulation

This section investigates the performance of each method in numerical simulations. Two ellipse targets are assumed in this case. Table 1 lists parameter values $\boldsymbol{P}$ for each target. The received data are generated by the geometrical optics

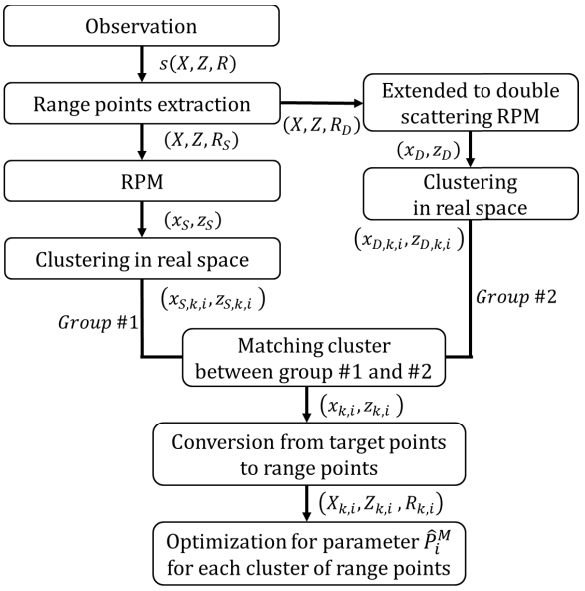

Fig. 3 Flowchart of the proposed method.

Table 1 Parameters $\boldsymbol{P}$ for each target.

Target	a[λ]	b[λ]	X_c[λ]	Z_c[λ]	θ[rad]
1	3.0	4.0	−15.0	10.0	$-\frac{2}{5}\pi$
2	2.6	4.0	15.0	10.0	$\frac{3}{5}\pi$

approximation, where the double-scattered components between wall and target or between target and target are considered. An omni-directional antenna scans along a circle of radius is 4λ centered at $(x,z) = (0,0)$. The number of observation samples is 100. Gaussian white noise is added to the received signals. Here, the S/N is defined as the ratio of peak instantaneous signal power to the averaged noise power, after applying the matched filter.

Figure 4 shows the results of ellipse fitting using the double- and single-scattered signals in real space [6] with S/N of around 30 dB. Here, the position of the wall is $(x,z) = (0, 20\,\lambda)$ and the simulated annealing algorithm [9] is employed to obtain a global optimum in Eq. (1) or (2), where the Levenberg Marquardt method is recursively used for local optimization. To emphasize the extrapolated boundary of the targets from a statistical viewpoint, another approach for image expression is used in this paper. This involves only imaging the region for which the focused region of the ellipse boundaries, obtained from the results of the simulated annealing, exceeds a certain threshold [6]. This figure shows that the extrapolated image is far from the actual ellipse because the RPM imaging error, enhanced by random noise, seriously influences the fitting process in real space. Figure 5 shows the result of ellipse fitting using the single-scattered signal in data space, specifically using the conventional method [6], and indicates that while the extrapolation accuracy is significantly enhanced, the reproduced target region is still small due to the use of only single-scattered components. In contrast, Fig. 6 shows the extrapolated image obtained using the double- and single-scattered signals

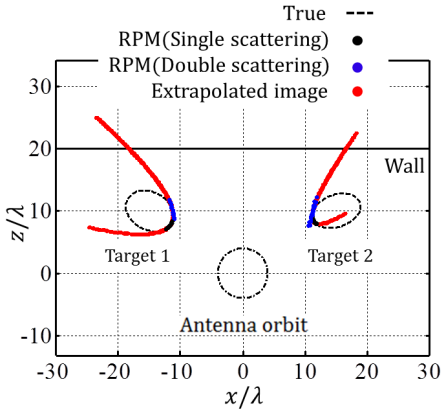

Fig. 4 Extrapolation in real space where single and double scattered signals are used.

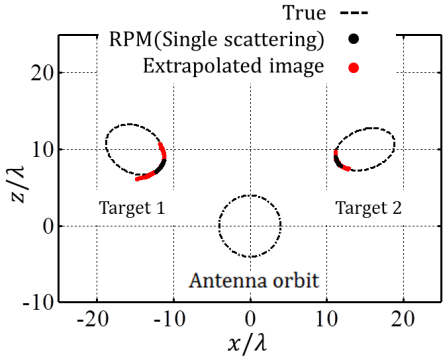

Fig. 5 Extrapolation in data space where single scattered signals are used, namely the conventional method.

in data space, and analyzed using the proposed method. This figure demonstrates that the proposed method can enhance simultaneously the extrapolation accuracy and expand the imaging region. This is because the fitting accuracy is impervious to imaging errors from the RPM method. To clarify this point, Fig. 7 shows the distribution for the ranges observed at each antenna location, namely, the distribution of data space in this case. This figure indicates that, while it is difficult to cluster range points for each target in data space using the correct clustering result in real space for the RPM image as in Fig. 6, clustering in data space becomes possible by exploiting the one-to-one correspondence between range point and target point.

Quantitative analysis for each method is investigated as follows. First, the extrapolation accuracy for the estimated image is defined as

$$\mathrm{e} = \min_{\boldsymbol{x}_{\mathrm{true}}} \left\| \boldsymbol{x}_{\mathrm{e}}{}^{i} - \boldsymbol{x}_{\mathrm{true}} \right\|, \quad (i = 1, 2, \ldots, N_{\mathrm{est}}) \tag{3}$$

where $\boldsymbol{x}_{\mathrm{true}}$ and $\boldsymbol{x}_{\mathrm{e}}{}^{i}$ represent the locations of the true and estimated target points, respectively, and N_{est} denotes the total number of estimated points. Also, for the assessment of the possible imaging region, the evaluation value $P_{\mathrm{a}} = (N'_{\mathrm{e}}/N_{\mathrm{true}}) \times 100\,[\%]$ is introduced, where N_{true} denotes the number of true target points and N'_{e} expresses the number of estimated target points that satisfy $\mathrm{e} \leq 0.1\,\lambda$. This index is also used in [10] for assessing the reconstructible ratio. Table 2 summarizes the values of $P_{\mathrm{a}}[\%]$ for the presumed image of each target in Figs. 5 and 6. These results quantitatively prove that the proposed method significantly expands the target image without reducing accuracy.

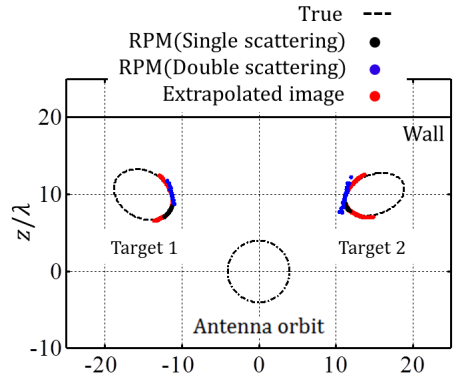

Fig. 6 Extrapolation in data space where single and double scattered signals are used, namely the proposed method.

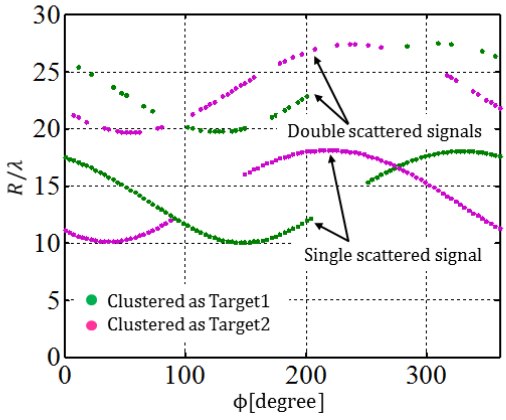

Fig. 7 Range points corresponding to each clustered RPM target points.

Table 2 Value of $P_a[\%]$ of each method at S/N = 30 dB.

Target	1	2
Conventional method (Fig. 5)	22.1	18.7
Proposed method (Fig. 6)	31.1	33.8

6. Conclusion

This paper proposed an image expansion method that exploits the double-scattered signals generated between target and walls, that arise in typical indoor environments. In this method, similar to the former approach, the range-points-based ellipse fitting scheme is adopted to avoid inaccuracies caused through RPM imaging. In addition, false images generated by double-scattered signals or other interference effects are significantly suppressed by employing the appropriate clustering algorithm for the image obtained by the single- and double-scattered components. The results from

numerical simulation based on the geometrical optics approximation showed that the proposed method remarkably expanded the imaging region compared with that obtained by the conventional method. This is mainly attributed to the use of the double-scattered components.

In this study, we only deal with the single- and double-scattered signals for imaging whereas higher-order multiply scattered signals actually occur. In general, the amplitudes for these higher-order signals are significantly lower compared with that for single- or double-scattering. Hence, these higher-order scatterings are considered to have less impact on performance of the proposed method. However, because this component includes independent information not obtainable from the single- and double-scattering component, future work will employ higher-order multiple scattering to improve extrapolation accuracy. Moreover, this paper only dealt with the 2-dimensional problem, where not ellipsoids but ellipses are used. The results obtained in this model can be adapted to a 3-dimensional model because in this method the extrapolation accuracy is dominated by the accuracy for range-point extraction, which is determined by the similarity between the transmitted and scattered signal because of Wiener filtering. We confirmed that the similarity of these waveforms is maintained in both 2- and 3-dimensions if the size of the target is sufficiently larger than wavelength; see [6]. Our intention is after extending this method to 3-dimensions, it is to be the basis for an experimental investigation.

References

[1] S. Kidera, T. Sakamoto, and T. Sato, "Accurate UWB radar three-dimensional imaging algorithm for a complex boundary without range points connections," IEEE Trans. Geosci. Remote Sensing, vol. 48, no. 4, pp. 1993–2004, Apr. 2010.

[2] Y. Abe, S. Kidera, and T. Kirimoto, "Accurate and omnidirectional UWB radar imaging algorithm with RPM method extended to curvilinear scanning model," IEEE Geosci. Remote Sens. Lett., vol. 9, no. 1, pp. 144–148, Jan. 2012.

[3] D. L. Mensa, G. Heidbreder, and G. Wade, "Aperture synthesis by object rotation in coherent imaging," IEEE Trans. Nucl. Sci., vol. 27, no. 2, pp. 989–998, Apr. 1980.

[4] R. Yamaguchi, S. Kidera, and T. Kirimoto, "Accurate imaging method for moving target with arbitrary shape for multi-static UWB radar," IEICE Trans. Commun., vol. E96-B, no. 7, pp. 2014–2023, July 2013.

[5] R. Salman and I. Willms, "3D UWB radar super-resolution imaging for complex objects with discontinous wavefronts," Proc. IEEE Int. Conf. Ultra Wideband 2011, Bologna, pp. 346–350, Sept. 2011.

[6] Y. Abe, S. Kidera, and T. Kirimoto, "Accurate image expansion method using range points based ellipse fitting for UWB Imaging Radar," IEICE Trans. Commun., vol. E95-B, no. 7, pp. 2424–2432, July 2012.

[7] S. Kidera and T. Kirimoto, "Fast and shadow region 3-dimensional imaging algorithm with range derivative of doubly scattered signals for UWB radars," IEEE Trans. Antenn. Propag., vol. 60, no. 2, pp. 984–996, Feb. 2012.

[8] P. Setlur, M. Amin, and F. Ahmad, "Multipath model and exploitation in through-the-wall and urban radar sensing," IEEE Trans. Geosci. Remote Sensing, vol. 49, no. 10, pp. 4021–4034, Oct. 2011.

[9] S. Kirkpatrick, C. D. Gelatt Jr., and M. P. Vecchi, "Optimization by simulated annealing," Science, vol. 220, no. 4598, pp. 671–680, May 1983.

[10] Y. Niwa, S. Kidera, and T. Kirimoto, "Image expansion approach for target buried in dielectric medium with extended rpm to multi-static UWB radar," IEICE Trans. Electron., vol. E96-C, no. 1, pp. 119–123, Jan. 2013.